SUSTAINABLE SYNTHESIS OF GOLD NANOPARTICLES FROM FRUIT WASTE AND THEIR POTENTIAL AS ANTIBACTERIAL AND ANTIOXIDANTS

Hitesh Rajput[1], Abhitosh Kedia[2*], Dimple Shah[3],

Abstract: In the present work, we employed an extracted solution of fruit waste (*Punica granatum and Artocarpus heterophyllus*) as an, environmentally friendly green synthesis method to synthesize gold nanoparticles with well-defined geometries at room temperature (30 °C) with distinctive structurally related optical properties. The phytochemicals present in the aqueous fruit extracts served as reducing agents along with the stabilization of nanoparticles. UV-visible spectroscopy measurement shows surface plasmon resonance in the visible region shows the formation of metal nanoparticles further in confirmation with Transmission Electron Microscopy (TEM) measurements and Dynamic Light Scattering (DLS) analysis used to examine the average size and shape of the particles. The Selected Electron Area Diffraction (SEAD) pattern indicated that the particles were crystalline with a face-centred cubic (fcc) structure. The stability of particles was determined through zeta potential. As-prepared nanoparticles were utilised further for antibacterial activity against *E. coli* and antioxidant activity in DPPH and ABTS.

Keywords: Punica granatum, Artocarpus heterophyllus, Gold, Transmission electron Microscope

[1, 2*]Department of Physics, Uka Tarsadia University, Bardoli, Surat-394350, Gujarat, India.
[1,3]Applied Physics Department, SVNIT, Surat, Gujarat, India.

***Corresponding Author**: Abhitosh Kedia
[2*]Department of Physics, Uka Tarsadia University, Bardoli, Surat-394350, Gujarat, India
abhitosh.kedia@utu.ac.in ; Tel: +91 8780357578

DOI: 10.53555/ecb/2022.11.9.158

Introduction:

Nanobiotechnology is currently the fastest-growing field within nanoscience and technology. Nanoparticles with an average size of 1-100 nm [1], spanning various spatial dimensions, are consistently synthesized through top-down and bottom-up approaches (Figure 1).

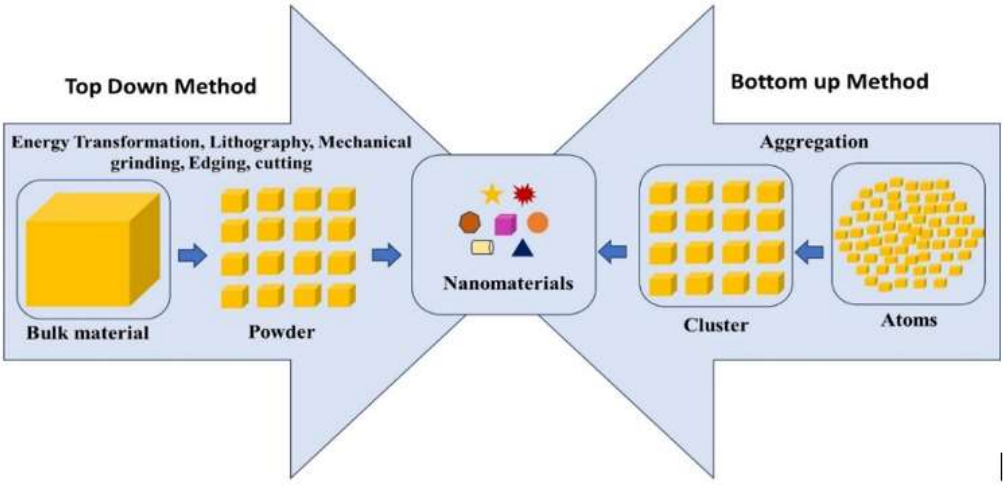

Figure 1: shows a schematic diagram of the top-down and bottom-up synthesis approach

The top-down method involves synthesizing nano-sized materials from bulk substances by providing mechanical energy, while the bottom-up method entails gathering atoms or molecules to create molecular structures of nanometer dimensions. Typically, the bottom-up approach is employed for the chemical and biological production of nanoparticles [2]. Due to their high surface-to-volume ratio, metal nanoparticles possess a novel property in terms of their physical, chemical, electronic, electrical, mechanical, magnetic, thermal, dielectric, optical, and biological characteristics when compared to larger bulk materials [3-4].

In nanotechnology, a crucial focus is on creating a more reliable method for synthesized nanomaterials that can be tunable in size and chemical composition across a broad spectrum. Precise management of size, shape, and crystalline structure has led to the use of nanotechnology in various fields [5-7]. There are various methods developed for the synthesis of metal nanoparticles such as physical, chemical, and biological methods among them the chemical method involves the use of hazardous chemicals, such as sodium borohydride, poly-N-vinyl pyrrolidone (PVP), tetrakishhydroxymethylphosphonium chloride (THPC), and hydroxylamine. The use of toxic chemicals in nanoparticle synthesis has been restricted in the biomedical field. On the other hand, the physical method involves Lithography, high thermal energy (solvothermal method), laser ablation and UV-irradiation which requires costly structure facility and more energy [8-9].As part of worldwide initiatives to reduce hazardous waste, the growing need for nanomaterials should be met with environmentally friendly synthesis methods. The use of toxic and environmentally harmful substances in the production of nanoparticles for biological purposes must be significantly reduced or eliminated when synthesized via the green method. Utilizing biological systems such as plants, bacteria, fungi, and other organisms offers eco-friendly processes for the green synthesis of nanoparticles [10-11]. The development and application of effective approaches, such as fruit waste or plant extract-delivered nanoparticles can lead to less toxic potencies. The product is more ecologically friendly in this approach as the synthesis processes are considerably more like those of natural processes. This also results in the acceptance of the fundamental ideas of "green synthesis," which minimises waste and pollution while utilising harmless resources. When compared to other biogenic sources, using plant or fruit extracts for nanoparticle synthesis is relatively simple because the biomolecules present in the extracts can serve as both reducing and stabilizing agents during the process [11,12]. The primary phytochemicals involved include terpenoids, carboxylic acids, flavones, ketones, amides, and aldehydes [13]. Flavones, organic acids, and quinones are water-soluble phytochemicals responsible for promptly reducing the metal ions. Gold nanoparticles are used extensively for highly

sensitive biomolecular detection, biolabeling, and as catalysts in chemical reactions, as well as for their antibacterial and anti-oxidant activity properties [14-16]. There are several benefits to the green synthesis of AuNPs, such as improved biocompatibility and simple scaling-up and reaction processes. Additionally, combining AuNPs with green reductants might lead to synergistic biological effects. Different parts of plants, including roots, stems, bark, leaves, and petals, can be used to cap and stabilize AuNPs during green synthesis [17]. Nevertheless, there is still a requirement for an economically feasible and environmentally friendly method for manufacturing gold nanoparticles. Nowadays, several studies have exploited plant and fruit waste extract to synthesize the AuNPs, which are summarised below.

TABLE 1: Green synthesis of gold nanoparticles by different plant and fruit extracts:

Plants	Size(nm)	Types	Shape	References
Ananas comosus	16	Leaves	Spherical	[18]
Dillenia indica	5-50	Leaves	Spherical	[19]
Mulberry	15-53	Leaves	Spherical	[20]
Garcinia mangostana	32	Fruit	Mostly spherical and some hexagonal and some triangular	[21]
Cardamom	5-10	Fruit	Spherical	[22]
banana	20	Fruit	Spherical	[23]

Various research has demonstrated that the extracted solution of the fruit waste plays a crucial role in shaping the development of metal nanoparticles [21-25]. The shape and size of nanoparticles are attributed to varied concentrations and assortments of biomolecules across different extracts.

The involvement of numerous biomolecules renders the biological reduction, formation, and expansion of nanoparticles in a highly intricate process [26].

Additionally, achieving control over the uniform morphology is challenging because of the presence of diverse biomolecules. Although extensive research has been conducted on producing nanoparticles in an environmentally friendly way [27]. Our goal is to develop a cost-effective, eco-friendly method for creating valuable gold nanoparticles for various uses.

The increasing need for bio-nanotechnology has directed our focus to use agricultural waste as a sustainable precursor for synthesizing AuNps.The synthesis of AuNps using extract of Punica *granatum and Artocarpus heterophyllus* fruit waste extract is presented in this study as a rapid, eco-friendly, and cost-effective method. Various spectroscopic and advanced microscopic techniques are utilized to examine the physicochemical properties of the AuNps.

Recorded UV-Vis spectra show the presence of nanoparticles. Transmission electron microscopy (TEM) is used to analyze the size, shape, and crystallinity of the synthesized gold nanoparticles. These nanoparticles remain stable for several months and show potential use for antioxidant activity and antibacterial activity as discussed.

Materials and Method:

Materials:

Hydrogen tetrachloroaurate (III) hydrate ($HAuCl_4$ $3H_2O$) (99.9%) was purchased from Sigma-Aldrich Chemicals. 2,2'-azino-bis (3-ethylbenzothiazoline-6-sulfonic acid) (ABTS), potassium persulfate (APS) and 2,2-diphenyl-1-picrylhydrazyl (DPPH) were bought from Sisco Research Laboratory PVT. LTD. While the *Punica granatum and Artocarpus heterophyllus* are from the local market of Bardoli town, India.

Preparation of the Fruit Waste Extract:

To prepare the *Punica granatum* extract *and Artocarpus heterophyllus*, the collected fruit waste was thoroughly washed with water several times to eliminate any remaining dust particles.

After cleaning, the leaves were dried under sunlight, the dried waste was crushed by a grinder to form a fine powder. A mixture of 5 g of the fine powder mentioned above and 100 ml of Millipore water was subjected to a 30-minute sonication at 60 °C (40 KHz). Afterwards, the mixture was passed through Whatman No. 1 filter paper, and the resulting filtered solution was kept at 4 °C for future use (Figure 2).

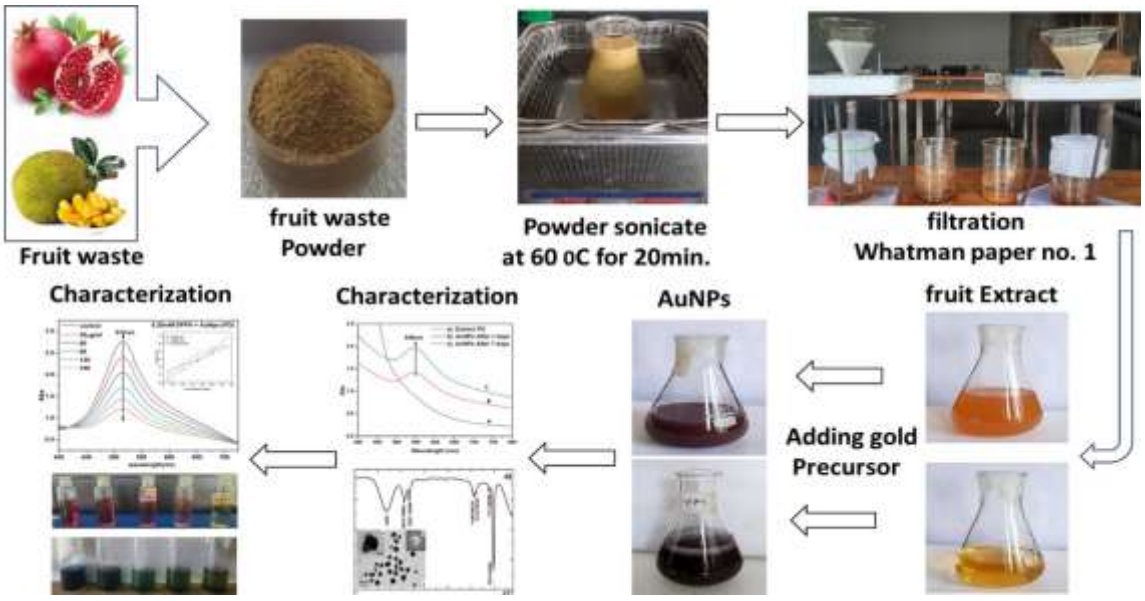

Figure 2: Schematic diagram of the synthesis process of AuNPs using fruit waste (*Punica granatum and Artocarpus heterophyllus*)

Green Synthesis of Gold Nanoparticles:

1 mM concertation of Hydrogen tetrachloroaurate (III) hydrate ($HAuCl_4.3H_2O$) precursor was added to 20 ml of the prepared fruit extract solution separately at room temperature while stirring (Figure 2) for four hours. The solution of color changed to dark pinkish. Afterwards, the resultant solutions were centrifuged thrice at 10,000 rpm in water at 10 ^{0}C and used for further characterization. The final concentration of formed NPs is calculated following a paper published by Xiong Liu et al. (Au Nps) [28] mentioned in the text.

Antioxidant Studies:

The assay for scavenging the 2,2-diphenyl-1-picrylhydrazyl (DPPH) free radical:

The DPPH assay was used to evaluate the antioxidant properties of AuNPs synthesized using fruit waste varying doses [29-30]. To conduct the assay, different amounts (50–300 µg/ml) of nanoparticles were mixed with 2 ml of a 0.25 mM methanolic solution of DPPH and left to incubate in the dark at room temperature for 30 minutes. Subsequently, the reduction in optical density at 517 nm, the characteristic peak of DPPH, was measured using UV-Vis spectroscopy, indicating a change in color from purple to yellow, signifying DPPH degradation as it received an electron from the nanoparticles [31]. The percentage inhibition for the DPPH radical scavenging activity was then determined using a specific formula.

$$\textit{Percentage inhibition} = \frac{(\textit{Control Abs.} - \textit{Sample Abs.})}{\textit{Control Abs.}} \times 100 \text{ ----------(1)}$$

Determination of 2,2'-azino-bis (3-ethylbenzothiazoline-6-sulfonic acid) (ABTS) radical cation scavenging activity:

The radical cation scavenging activity of AuNPs obtained from Fruit waste was assessed using the ABTS assay. To create ABTS radical cations, a mixture of 10 mM ABTS and 3.5 mM APS (potassium persulfate) was allowed to incubate in the dark at room temperature for 16 hours. Subsequently, the mixture of ABTS Assay and different concentrations (50–300 µg/ml) of synthesized AuNPs was incubated in the dark for 10 minutes at room temperature. Following the incubation, the activity was determined spectrophotometrically by observing the change in colour from blue-green to light green or colourless, which led to a reduction in optical density, and then the absorbance at 745 nm was measured using a UV Vis spectrophotometer. The equation (1) was used to calculate the percentage of radical cation scavenging activity. The results obtained were then compared with the antioxidant activity of standard Ascorbic acid at the same concentration range of 50-300 µg/ml.

Antibacterial Activity:

The efficiency of the synthesized AuNPs in inhibiting bacterial growth was evaluated using the agar well diffusion method. Initially, the Escherichia coli strain no ACCC 8739 was cultured in a nutrient broth for 24 hours at 310K. A 100 µl portion of the young E. coli culture was then mixed with a sterile 100 ml nutrient agar medium to prepare plates. Subsequently, 6 mm wells were created in the agar plates to introduce the

nanoparticles. Different volumes (25, 50, 100, and 200 microliters) of the synthesized AuNPs (at a concentration of 400 µM) were used to test their antibacterial activity against *E. coli*. The inoculated plates were then kept at 310 K for 24 hours. After the incubation period, the zone of inhibition was observed and measured. For positive control, the plate was prepared with Colistimethate (400 µM).

Characterization Techniques:

We conducted optical absorption measurements on our nanoparticle solution samples using a Thermo Scientific absorption spectrophotometer in the wavelength range of 300-1100nm. TEM samples were prepared by drying the centrifuged samples in water on copper grids coated with carbon formvar, and we obtained images using the FE-Technai G^2 system operated at an accelerating voltage of 300kV. FT-IR spectroscopy, performed on Bruker alpha in the transmission mode (600-4500) cm^{-1}. Particle surface charge and particle size analysis were performed using the Malvern Zetasizer (Nano-ZS 90). All measurements were carried out at room temperature unless stated otherwise.

Result and Discussion:

For the green synthesis of AuNPs, *Punica granatum (PG) and Artocarpus heterophyllus (AH)* extract were added to a solution of gold chloride trihydrate, and the reaction commenced within a few minutes, leading to a color change in the mixture. The formation of AuNPs was initially verified by the change in color from colourless to a dark pinkish within 30 minutes, indicating the formation of Au NPs giving rise to surface plasmon resonance, a collective movement of the surface electrons in the conduction band of metal nanoparticles in the visible region.

In PG-AuNPs (Figure 3a), a distinct single surface plasmon band, centred around 546 nm, is observed, while AH-AuNPs exhibit broad bands in the 550-590 nm range, as depicted in Fig. 3b. This observation represents a critical characteristic of the geometrical metal nanostructures. The presence of a single but slightly broad peak, resembling a Gaussian curve, in Punica Granatum indicates the presence of monodisperse anisotropic nanoparticles. However, the deviation from spherical geometry is not significant, as confirmed by the TEM images (Figure 4).

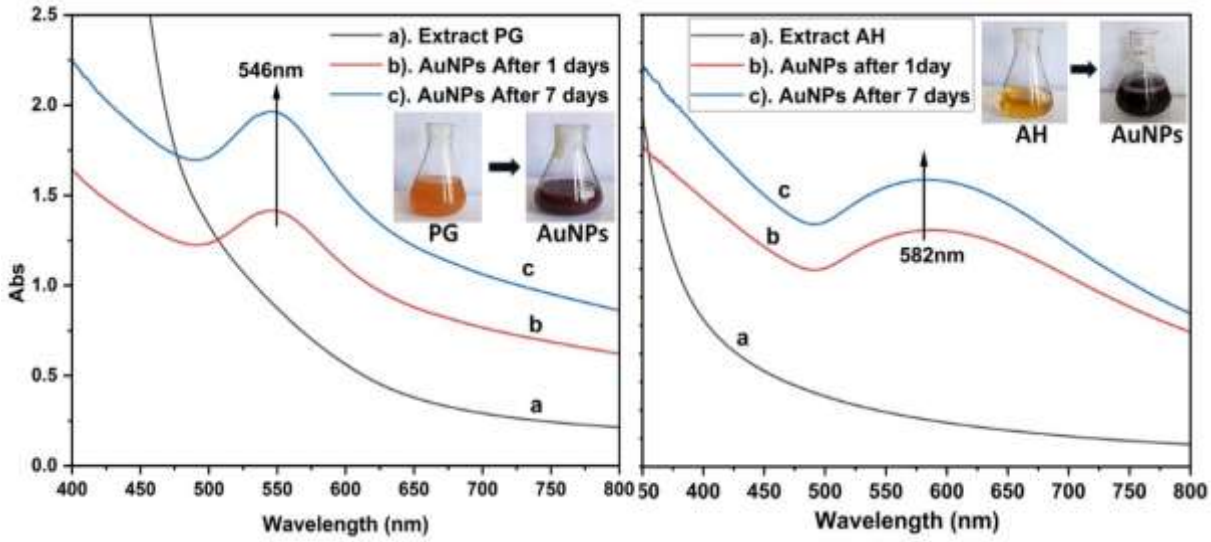

FIGURE 3: UV- Vis. spectra of formed Gold nanoparticles in a) *Punica Granatum* and b)*rtocarpus heterophyllus* over a period indicates the formation of stable nanostructures.

From TEM images, we determined that the average size of the nanoparticles from Punica Granatum was approximately 50 to 70 nm (Figure 4a), while the quasi-spherical Au nanoparticles from Artocarpus heterophyllus were polydisperse in size with an average size of 22 nm (Figure 4a').

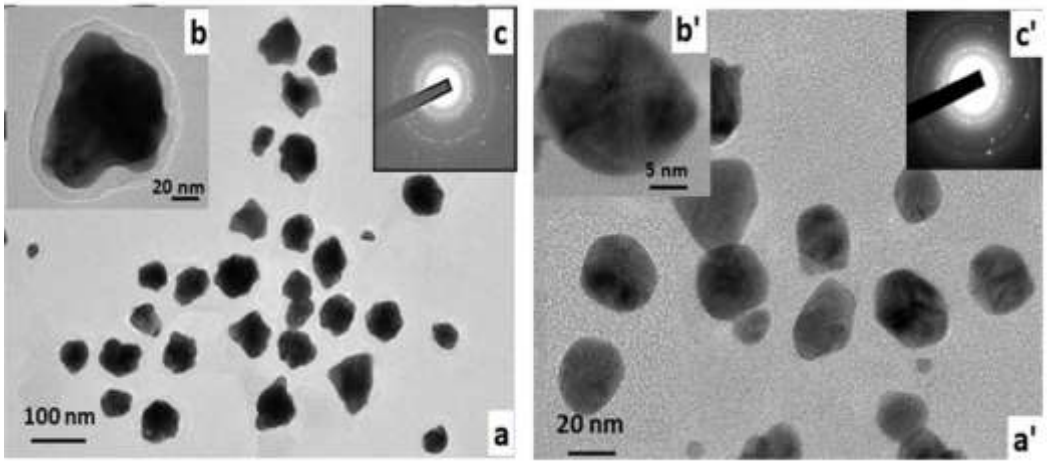

FIGURE 4: TEM images of formed AuNPs in a) Punica Granatum and a') Artocarpus heterophyllus.

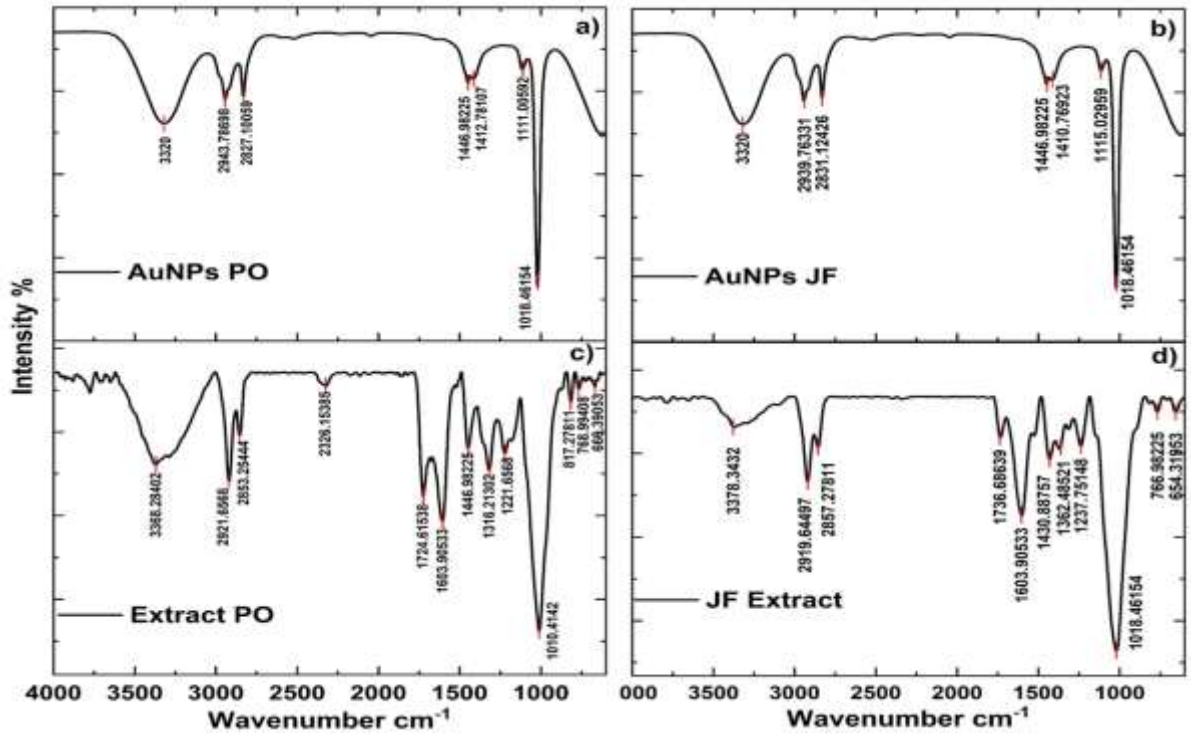

Figure 5: FTIR spectra of a) PG-AuNPs and b) AH-AuNPs c) *Punica Granatum* extract d) *Artocarpus heterophyllus* extract.

The FTIR spectrum of the *Punica Granatum* and *Artocarpus heterophyllus* extract before and after the synthesis of AuNps (Figure 4) and the exitance peak of the band is shown in below Table 2.

Table 2: Present and missing band in fruit waste extract and synthesised AuNPs [23].

Punica Granatum Band (cm^{-1})	PG-AuNPs Band (cm^{-1})	*Artocarpus heterophyllus* Band (cm^{-1})	AH-AuNPs Band (cm^{-1})	Attribute of group present due to band
666.39	Missing	654.3319	Missing	
768.99	Missing	786.98	Missing	Cis =C–H out-of-plane bending
1010.41	1018.64	1018.46	1018.46	C-C and C-O vibration of carbohydrate
1316.21	1412.78	1237.78	1410.76	–OH, bending vibrations

1446.98	1446.98	1430.88	1446.98	C-H bending vibration
1603.90	Missing	1603.90	Missing	C–C skeletal vibrations
1724.61	Missing	1763.68	Missing	–C=O stretching vibrations
2921.65	2943.78	2919.64	2939.76	C-H starching
3368.28	3320	3375.34	3320	Stretching of (O-H) group

The analysis of the spectrum revealed that some bands found in fruit waste extract have disappeared and shifted with the synthesized AuNPs. This suggests that certain groups (like carboxylic acids, flavones, ketones, amides, and aldehydes) present in the fruit extract actively contribute to the reduction, stabilization, and capping of agents during the synthesis of AuNPs.

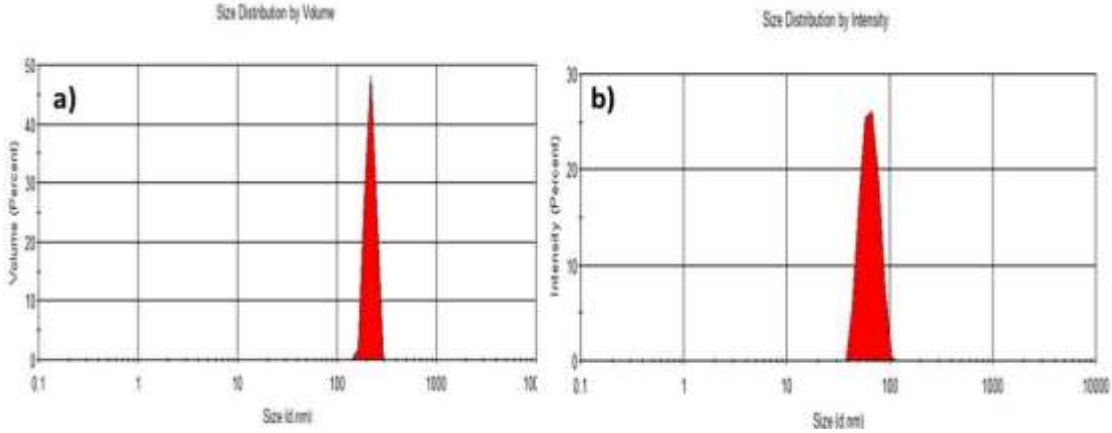

Figure 6: DLS spectra of synthesized AuNPs using a) *Punica Granatum b) Artocarpus heterophyllus.*

DLS measurement for the good distribution solution of AuNPs indicated the average particle size of 218 nm in *Punica Granatum* and 65 nm in the case of *Artocarpus heterophyllus* (Fig.6). Size obtained in DLS was greater compared to the size seen in TEM images likely due to impact of the dispersant on the hydrodynamic diameter agglomeration of the nanoparticles [31].

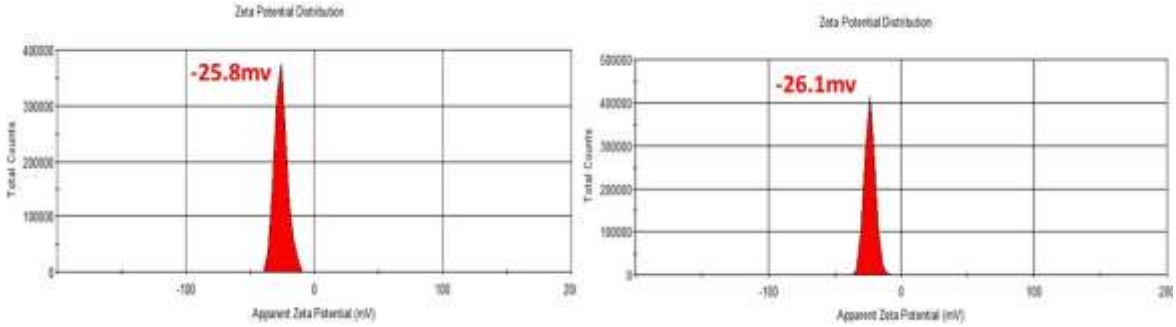

Figure 7: Zeta Potential of synthesized AuNPs using a) *Punica Granatum b) Artocarpus heterophyllus*

Zeta potential values serve as a key indicator of the stability of colloidal particles. These absolute values reflect the overall electrical charge on the external surface of the particles, which is a result of the surface functional groups. Nanoparticles are

classified as stable colloids if their zeta potential exceeds 25 mV or falls below –25 mV [33]. In this case, Figures 7a & 7b show the Zeta potential of the green synthesised AuNPs with a sharp peak at -25.8 mV and -26.1 mV in *Punica Granatum* and *Artocarpus heterophyllus*, respectively. The negatively charged surface of the NPs in the dispersed medium was confirmed by the negative value of the zeta potential, and the repulsion among the particles made them stable.

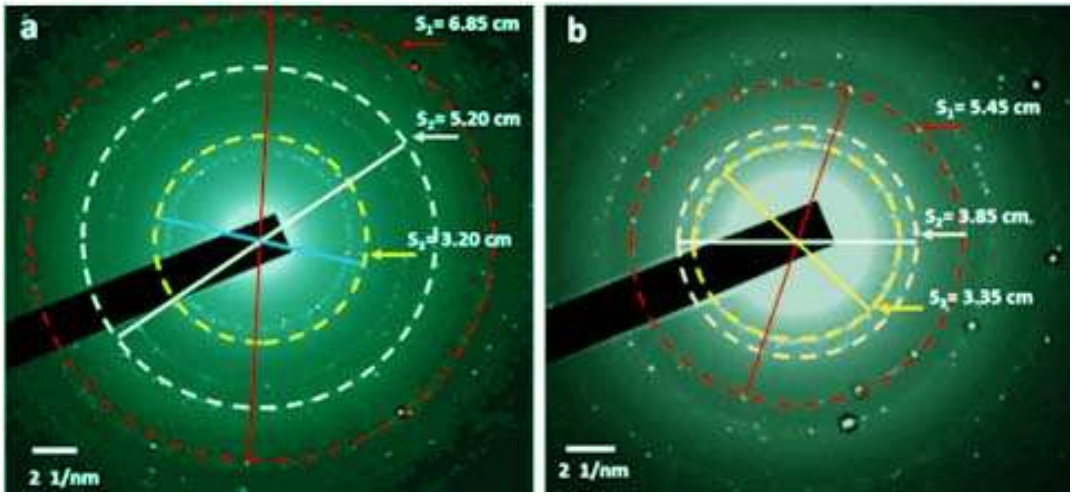

Figure 8: SEAD pattern of synthesized AuNPs using a) *Punica Granatum and b) Artocarpus heterophyllus with calculating the diameter of rings.*

The structural information of the particles was also obtained from the selected area electron diffraction (SAED) pattern, as shown in Figure 8. Typically, the respective d-spacing of the particles was determined by calculating the diameter of the different rings using the formula-1 [33].
(diameter/2) (mm, divided by 2 for 2 spot): (1/d1) (1/nm) = (mm, the rule bare length) :(1/nm)

This formula was employed to calculate d-spacing d1, d2, and d3, as indicated in table 3. Upon comparison of this data with the JCPDS standard data file number-00-004-0784, we identified crystalline planes (111), (220), (400), and (200) correspondingly. As a result, we can infer that AuNPs possess a face-centred cubic structure.

TABLE 3: d spacing calculated from the above formula matches with JCPDS standard data file number 00-004-0784 of Au indicating crystalline FCC structure.

	d1(nm)	**hkl**	**d2(nm)**	**hkl**	**d3(nm)**	**hkl**
Punica Granatum	1.0194	(400)	1.4423	(220)	2.3537	(111)
Artocarpus heterophyllus	1.4406	(220)	2.0426	(200)	2.3560	(111)

Figure 9: *Antibacterial activity of synthesized nanoparticles against the disease-causing E. coli; a) Colistimethate b), PG- AuNPs and, c) AH-AgNPs.*

The antimicrobial activity of the synthesized AuNPs against the *E. coli* (ACCC 8739) strain was assessed using the well-diffusion method.

The assessment involved measuring the diameter of the zone of inhibition surrounding the wells containing the synthesized nanoparticles. E. coli inhibition was observed at varying doses of AuNPs (25 µl, 50 µl, 100 µl, and 200 µl) of concentration 400 µM. The results of the antibacterial test can be seen in Figure 9. These results were compared with those of the standard drug Colistimethate (400 µM). An increase in the volume of synthesized NPs resulted in an expansion of the diameter of the zone of inhibition (Table 4).

Table 4: Zone of inhibition as per NPs dose in volume.

Material	**Zone of inhibition**			
	25 µl	50 µl	100 µl	200 µl
Colistimethate	-------	9 ± 0.25mm	12±0.25mm	13±0.25mm
PG-AuNPs	7 ± 0.25mm	8 ± 0.25mm	10±0.25mm	12±0.25mm
AH-AuNPs	7 ± 0.25mm	8 ± 0.25mm	10±0.25mm	11±0.25mm

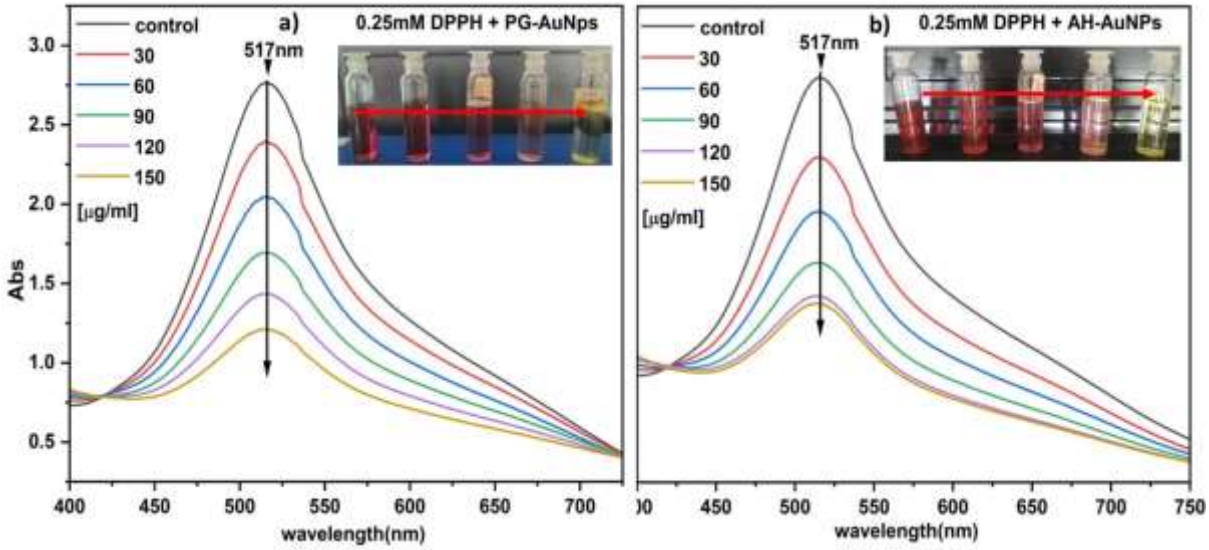

Figure 10: Antioxidant activity of AuNPs synthesized by a). Punica Granatum and b) Artocarpus heterophyllus against DPPH.

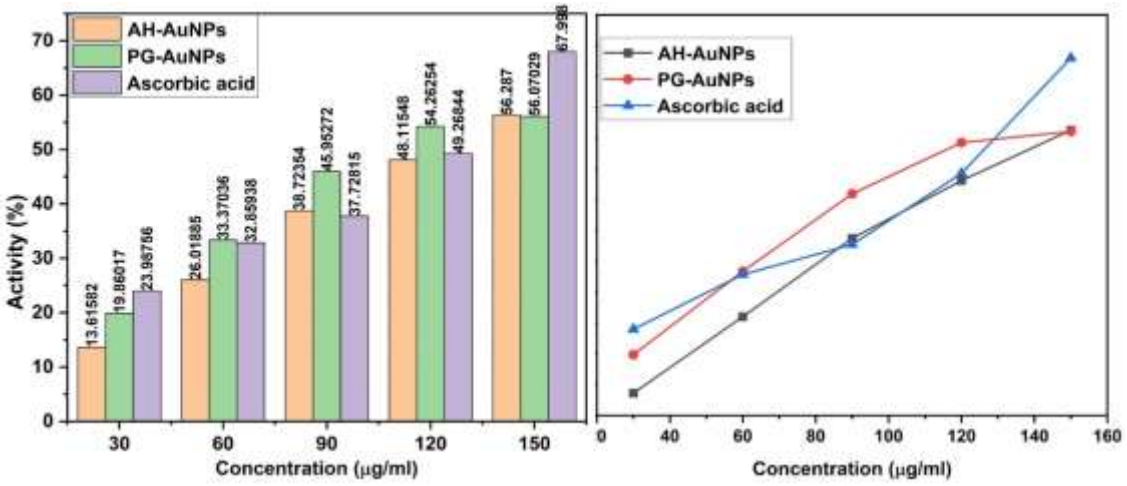

Figure 11: Antioxidant activity of AuNPs synthesized by Punica Granatum and Artocarpus heterophyllus against DPPH a) Bar Graph b). activity curve compares with ascorbic acid activity.

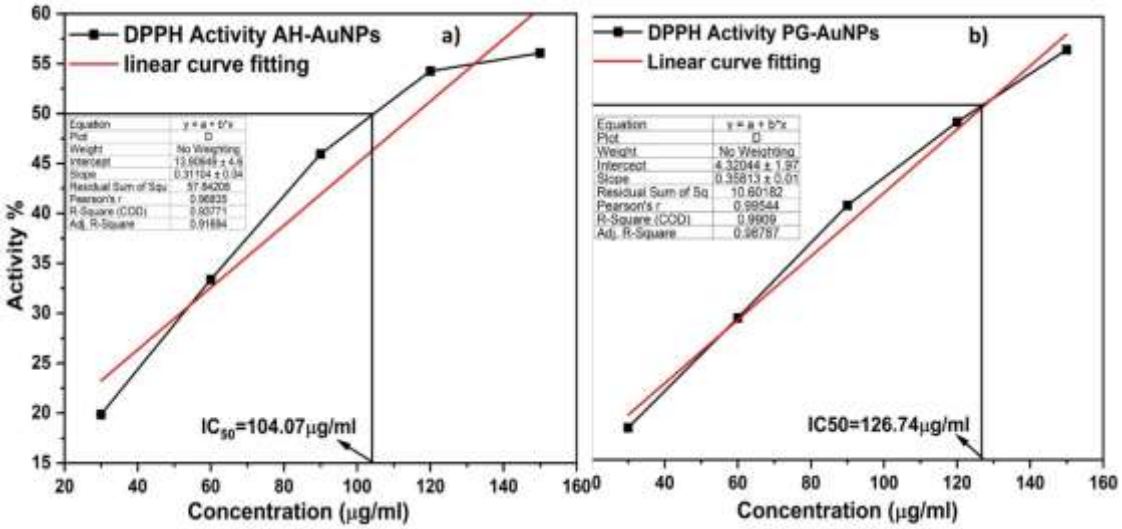

Figure 12: IC50 value of the *Antioxidant activity of AuNPs synthesized by a). Punica Granatum and b) Artocarpus heterophyllus against DPPH*

.

Metallic nanoparticles, which act as antioxidants, play a significant role in combatting harmful free radicals like DPPH and ABTS, a commonly detrimental free radical. Regarding the mechanism of the DPPH assay, it was established that by receiving an electron or a hydrogen atom from MNPs, DPPH was eliminated, converting the OH-DPPH solution into the non-radical form of DPPH-H [35]. The results regarding the influence of different concentrations of AuNPs on the DPPH radical scavenging activity can be seen in Figures 10a and 10b. DPPH degradation exhibited antioxidant activity that depended on the dose, as the nanoparticle concentration increased, and the % inhibition also increased (Figure 11). DPPH is a stable molecule that can accept either electrons or hydrogen from AuNPs. DPPH is a stable molecule capable of accepting either electrons or hydrogen from AuNPs. Both PG-AuNPs and AH-AuNPs exhibited a high DPPH radical scavenging efficiency of about 56.28% and 56.07% respectively at a concentration of 150 µg/ml. In comparison, the standard antioxidant agent (Ascorbic acid) showed 67.98% efficacy at the same dosage (Figure 9). The IC50 values of PG-AuNPs and AH-AuNPs were determined to be 126.74µg/ml (Figure 11b) and 104.07 µg/ml (Figure 12a and 12b) respectively by plotting perpendicular lines to the x-axis from the 50% inhibition point (y-axis).

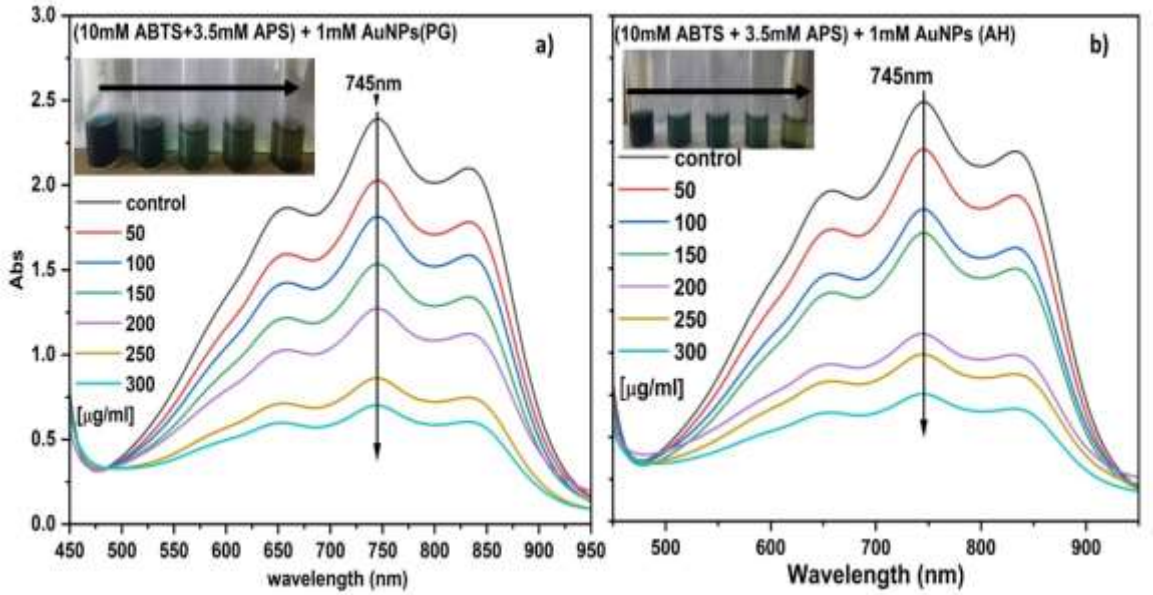

Figure 13: *Antioxidant activity of AuNPs synthesized by a). Punica Granatum and b) Artocarpus heterophyllus against ABTS.*

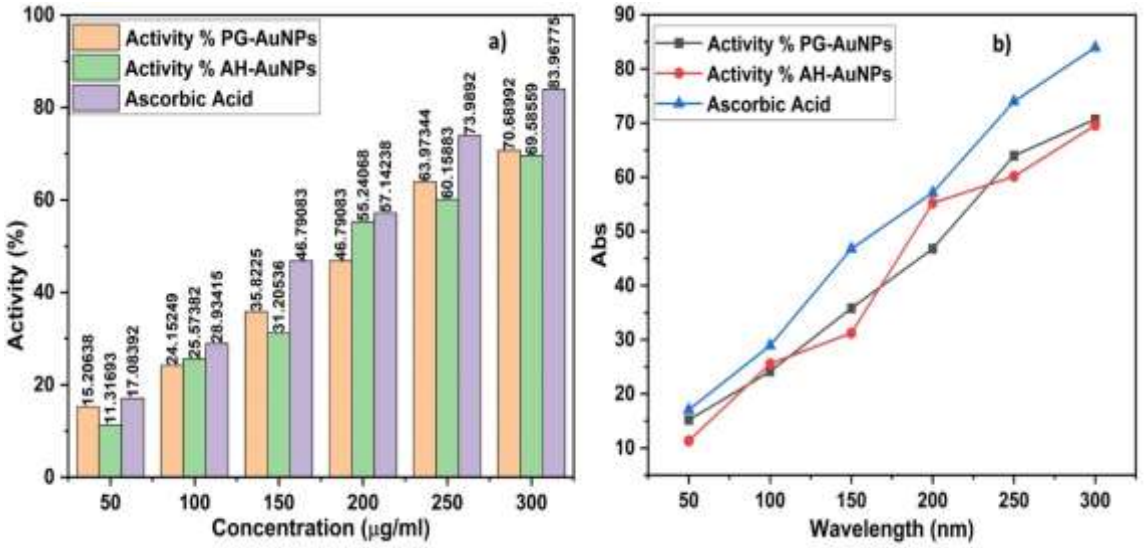

Figure 14: *Antioxidant activity of AuNPs synthesized by Punica Granatum and Artocarpus heterophyllus against ABTS a) Bar Graph b). activity curve compares with ascorbic acid activity.*

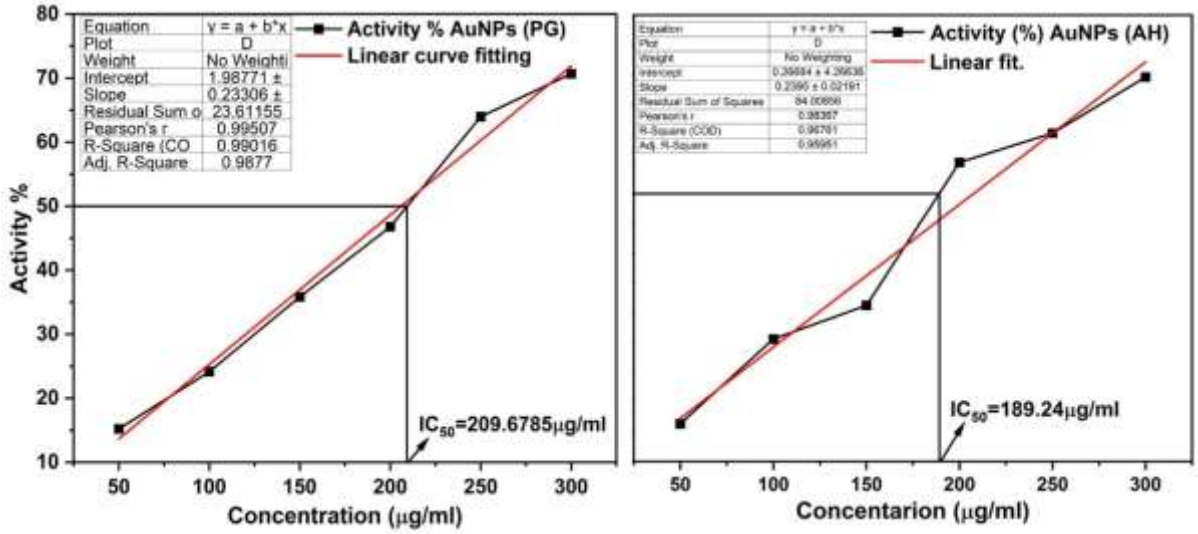

Figure 15: IC50 value of the *Antioxidant activity of AuNPs synthesized by a). Punica Granatum and b) Artocarpus heterophyllus against ABTS.*

During ABTS radical scavenging activity, ABTS undergoes conversion into a free radical cation by being oxidized with the assistance of the oxidation agent APS (potassium persulfate). This process involves allowing the mixture to react for approximately 16 hours, resulting in the formation of a stable blue-green ABTS·+ radical cation. Upon the introduction of AuNPs into the ABTS•+ solution, there is an electron or hydrogen atom transfer to the radical cation, causing its transformation into its colourless neutral form (ABTS) [36]. Consequently, this transformation leads to a decrease in absorbance, which can be measured using spectrophotometric analysis. It was observed that green-synthesized AuNPs demonstrated considerable ABTS free radical scavenging capability in a concentration-dependent manner.

As the concentration increased, the radical scavenging activity also showed a percentage increase, as depicted in Figures 13a and 13b. Within the concentration range of 50-300 µg/ml, an inhibition of 15-70% was observed, as shown in Figure 14. The IC_{50} value of PG-AuNPs and AH-AuNPs were determined to be 209.67 µg/ml (Figure. 15a) and 189.24 µg/ml (Figure. 15b) by drawing perpendicular lines to the x-axis from the point of 50% inhibition on the y-axis.

Conclusions:

Conclusively, we have effectively synthesized gold nanoparticles (AuNps) from the discarded fruit material of *Punica Granatum* and *Artocarpus heterophyllus* at room temperature via an environmentally friendly green synthesis approach. By utilizing waste material, the method

has become cost-effective and has yielded stable crystalline gold nanoparticles. The formation and stability of Au NPs were confirmed by UV-Vis and zeta potential spectral studies. Through TEM and DLS analysis, the average particle size was determined to be 50-70nm and 20-25 nm in *Punica Granatum* and *Artocarpus heterophyllus*, respectively. Calculation from SAED pattern showing FCC gold nanostructure. The IC50 values of PG-AuNPs and AH-AuNPs were determined to be 126.74µg/ml and 104.07 µg/ml in DPPH whereas 209.67 µg/ml and 189.24 µg/ml in ABTS. Further, the synthesized AuNps enhanced antibacterial activity against Gram positive bacteria.

Acknowledgements:
The authors are grateful to Uka Tarsadia University for materials characterization facilities and funding through RPS-UTU/RPS/1262/2018.

References:

1. Mahmoud Nasrollahzadeh, S. Mohammad Sajadi, Mohaddeseh Sajjadi and Zahra Issaabadi, Interface Science and Technology, Vol. 28. doi.org/10.1016/B978-0-12-813586-0.00001-8
2. Paulo F. M. de Oliveira, Roberto M. Torresi, Franziska Emmerling and Pedro H. C. Camargo, J. Mater. Chem. A, **8**, 16114–16141, (2020). DOI: 10.1039/d0ta05183g
3. Nadeem Baig, Irshad Kammakakam, and Wail Falath, Mater. Adv., **2**, 1821–1871, (2021). DOI: 10.1039/d0ma00807a.
4. Ibrahim Khan, Khalid Saeed, Idrees Khan, Arabian Journal of Chemistry, **12**, 908–931, (2019). doi.org/10.1016/j.arabjc.2017.05.011.
5. J. Spadavecchia, S. Casale, J. Landoulsi, Claire-Marie Pradier, chemical physics letters, **609**, 134-141, (2014). DOI:10.1016/j.cplett.2014.06.008.
6. S. Barbosa, A. Agrawal, I. Pastoriza-Santos, L. Rodr´ıguezlorenzo, R. A. Alvarez-Puebla, A. Kornowski, H. Weller, and L. M. Liz-Marz´a., Langmuir, **26**, 14943, (2016).
7. Saverot S, Geng X, Leng W, Vikesland P, Grove T, Bickford L., Facile, tunable, and SERS enhanced HEPES gold nanostars, RSC Adv. **6**, 29669- 29673, (2016). doi.org/10.1039/C6RA00450D
8. P. Raveendran, J. Fu and S. L. Wallen, J. Am. Chem. Soc., **125** (46), 13940–13941 (2003). doi: 10.1021/ja029267j.
9. K. B. Narayanan and N. Sakthivel, Adv. Colloid Interface Sci., **156**, 1–13, (2010). doi:10.1016/j.cis.2010.02.001.
10. N. N. Dhanasekar, G. R. Rahul, K. B. Narayanan, G. Raman, and N. Sakthivel, *J Microbiol Biotechnol* **25** (7), 1129–1135, (2015). doi:10.4014/jmb.1410.10036.
11. P. Singh, Y.-J. Kim, D. Zhang, and D.-C. Yang, Trends in Biotechnology, **34** (7), 588-599, (2016). doi: 10.1016/j.tibtech.2016.02.006.
12. S. Ahmed and S. Ikram, Nano Res Appl., **1,** 1-5, (2015). doi.org/10.1016/j.jrras.2015.06.006
13. Nehil Shreyash, Sushant Bajpai, Mohd. Ashhar Khan, Yashi Vijay, Saurabh Kr Tiwary, and Muskan Sonker, ACS Appl. Nano Mater., **4**, 11428-11457, (2021). doi.org/10.1021/acsanm.1c02946.
14. J. Singh, T. Dutta, Ki-Hyun Kim, M. Rawat, P. Samddar and P. Kumarr, J. of nanobiotechnology, **16**(84),1-24, (2018). doi.org/10.1186/s12951-018-0408-4
15. P. Vijaya Kumar, S. Mary Jelastin Kala, and K. S. Prakash, Rasayan J Chem, **11**, 1544-1551, (2018). doi.org/10.31788/RJC.2018.1144044
16. A. Aljabali ,y akkam, m. s. al zoubi , k. m. Al-batayneh , b. al-trad, o. abo alrob , a. m. Alkilany, m. benamara and d. j. Evans, Nanomaterials (Basel), **8**(3), 174, (2018). doi.org/10.3390/nano8030174.
17. K Adavallan and N Krishnakumar, Advances in Natural Sciences: Nanoscience and Nanotech., **5**(2):025018, (2014). DOI:10.1088/2043-6262/5/2/025018.
18. M.R. Bindhu, M. Umadevi, Materials Letters **120**, 122–125, (2014). doi.org/10.1016/j.matlet.2014.01.108.
19. Arghya Sett, Manoj Gadewar, Pragya Sharma, Manab Deka and Utpal Bora, Adv. Nat. Sci.: Nanosci. Nanotechnol. **7**, 025005, (2016). doi:10.1088/2043-6262/7/2/025005.
20. K. X. Lee, K. Shameli, M. Miyake, N. Kuwano, N. B. Bt Ahmad Khairudin, S. E. Bt Mohamad, and Yen Pin Yew, Journal of nanomaterials 1-7, (2016). doi.org/10.1155/2016/8489094.
21. L. Qiana, W. Sub, Y. Wangb, M. Dangc, W. Zhangc and C. Wangd, Nanomedicine, and Biotechnology, **47**(1), 1173-1180, (2019).
22. Veronika Soshnikova, Yeon Ju Kim, Priyanka Singh, Yue Huo, Josua Markus, Sungeun Ahn, Verónica Castro-Aceituno, Jongpyo Kang, Mohan Chokkalingam, Ramya Mathiyalagan & Deok Chun Yang, Artificial Cells, Nanomedicine, And Biotechnology, **46**(1), 108–117, (2018). doi.org/10.1080/21691401.2017.1296849.
23. Girish K. Deokar and Arun G. Ingale, RSC Adv., 6, 74620, (2016). DOI:10.1039/c6ra14567a.

24. K. Gopinath, S. Gowri, V. Karthika, A. Arumugam, J Nanostructure Chem. **4**, 115, (2014) DOI 10.1007/s40097-014-0115-0.
25. Kumar H, Bhardwaj K, Dhanjal DS, Nepovimova E, Ṣen F, Regassa H, Singh R, Verma R, Kumar V, Kumar D, Bhatia SK, Kuča K., Int J Mol Sci., **21**(22), 8458, (2020) doi:10.3390/ijms21228458.
26. J. Patra and K. H. Baek, *Journal of Nanomaterials*, 1-13, (2014).
27. Siavash Iravan, Green Chem., 2011, 13, 2638. DOI: 10.1039/c1gc15386b.
28. Xiong Liu, Mark Atwater, Jinhai Wang, Qun Huo; Colloids and Surfaces B: Biointerfaces **58**, 3–7, (2007). doi:10.1016/j.colsurfb.2006.08.005.
29. Mohamed Hosny, Abdelazeem S. Eltaweil, Mohamed Mostafa, Yaser A. El-Badry, Enas E.Hussein, Ahmed M. Omer, and Manal Fawzy; ACS Omega, **7**, 3121-3133, (2022). doi.org/10.1021/acsomega.1c06714.
30. Fazli Khuda, Meshal Gul, Atif Ali Khan Khalil, Sajid Ali, Naveed Ullah, Muhammad Shafiq Khan, Shabnam Nazir, Sumaira Irum Khan, Sultan Mehtap Büyüker, Saud Almawash, Muhammad Shafique, and Sayed Afzal Shah, ACS Omega, **8**, 30221-30230, (2023). doi.org/10.1021/acsomega.3c02928.
31. Elena N. Hristea, Miron T. Caproiu, Gabriela Pencu, Mihaela Hillebrand, Titus Constantinescu and Alexandru T. Balaban, Int. J. Mol. Sci, **7**, 130-143, (2006). doi.org/10.3390/i7050130.
32. T. G. F. Souza1, V. S. T. Ciminelli, N. D. S. Mohallem, Journal of Physics: Conference Series 733, 012039, (2016). doi:10.1088/1742-6596/733/1/012039.
33. Hiemenz, P.C.; Rajagopalan, R. Principles of Colloid and Surface Chemistry, 3rd ed.; Marcel Dekker: New York, NY, USA, 650, (1997).
34. http://folk.ntnu.no/yingday/NilsYD/TEMCCD basic/DiffINdexing.pdf
35. Elena N. Hristea, Miron T. Caproiu, Gabriela Pencu, Mihaela Hillebrand, Titus Constantinescu and Alexandru T. Balaban, Int. J. Mol. Sci. **7,** 130-143, (2006). doi.org/10.3390/i7050130.
36. Savan Donga, Gopala Ram Bhadu & Sumitra Chanda, Artificial Cells, Nanomedicine, and Biotechnology, **48(**1),1315-1325, (2020). DOI:10.1080/21691401.2020.1843470.